Supplementary Information

Mn 2*p* Resonant X-ray Emission Clarifies the Redox Reaction and Charge-Transfer Effects in $LiMn_2O_4$

Daisuke Asakura,[*a,b] Yusuke Nanba,[a,†] Eiji Hosono,[a,b] Masashi Okubo,[a,#] Hideharu Niwa,[c,d,$] Hisao Kiuchi,[e,§] Jun Miyawaki,[c,d] and Yoshihisa Harada[b,c,d]

[a]*Research Institute for Energy Conservation, National Institute of Advanced Industrial Science and Technology, Tsukuba, Ibaraki 305-8568, Japan*

[b]*AIST-UTokyo Advanced Operando-Measurement Technology Open Innovation Laboratory (OPERANDO-OIL), National Institute of Advanced Industrial Science and Technology (AIST), Kashiwa, Chiba 277-8565, Japan*

[c]*Institute for Solid State Physics, The University of Tokyo, Kashiwa, Chiba 277-8581, Japan*

[d]*Synchrotron Radiation Research Organization, The University of Tokyo, Sayo, Hyogo 679-5148, Japan*

[e]*Department of Applied Physics, The University of Tokyo, Bunkyo, Tokyo 113-8656, Japan*

* **Corresponding author**: Daisuke Asakura

Email address: daisuke-asakura@aist.go.jp, Tel: +81-29-861-0572, Fax: +81-29-861-5648,

Address: Research Institute for Energy Conservation, National Institute of Advanced Industrial Science and Technology, Tsukuba, Ibaraki 305-8568, Japan

Present Addresses

[†]Yusuke Nanba: Center for Green Research on Energy and Environmental Materials, National Institute for Materials Science, Tsukuba, Ibaraki 305-0044, Japan.

[#]Masashi Okubo: Department of Chemical System Engineering, The University of Tokyo, Bunkyo, Tokyo 113-8586, Japan.

[$]Hideharu Niwa: Faculty of Pure and Applied Sciences, University of Tsukuba, Tsukuba, Ibaraki 305-8571, Japan.

[§]Hisao Kiuchi: Office of Society-Academia Collaboration for Innovation, Kyoto University, Sayo, Hyogo 679-5198, Japan.

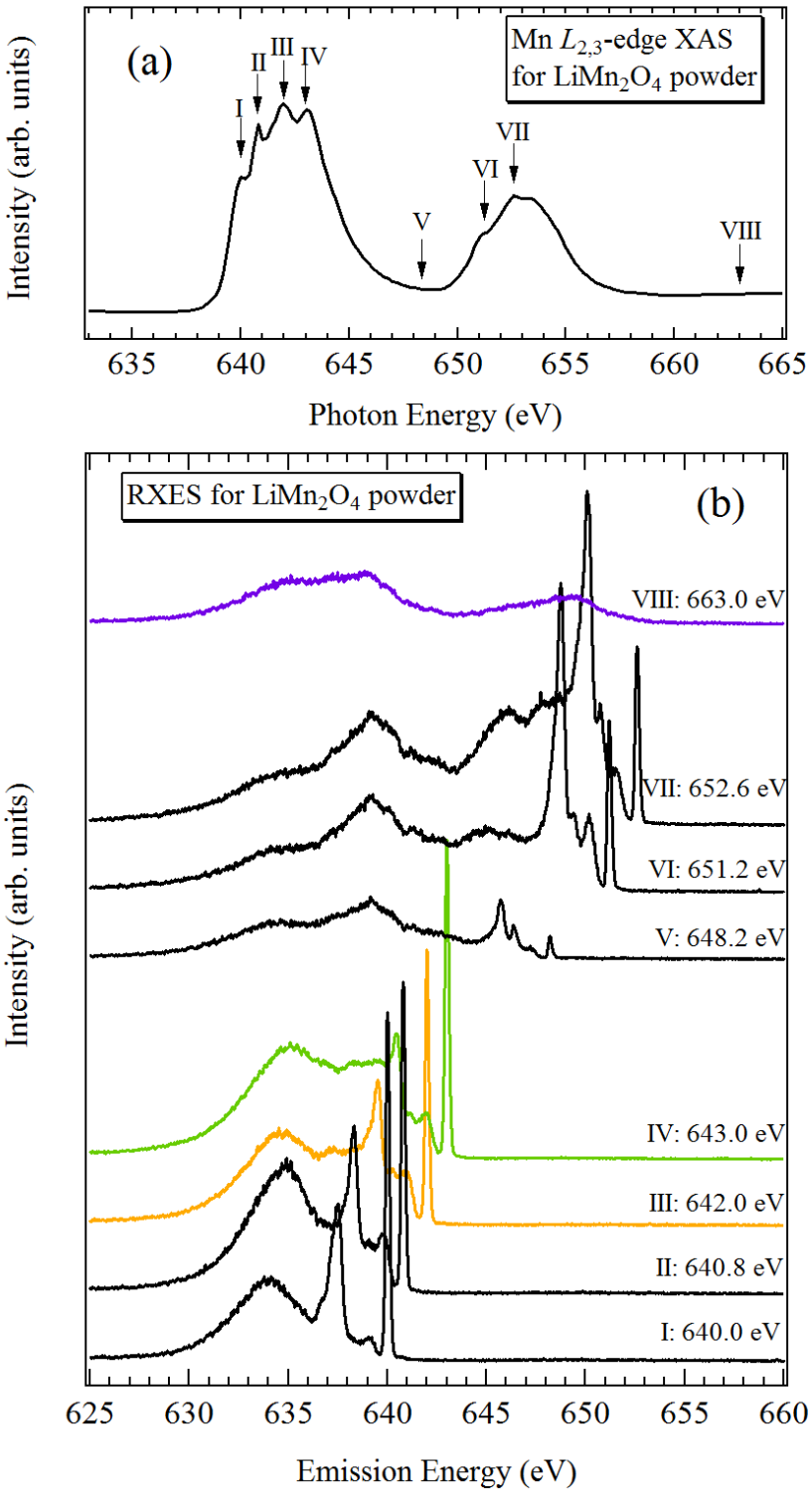

Fig. S1. (a) Mn $L_{2,3}$-edge TEY XAS and (b) XES for $LiMn_2O_4$ powder. For (b), the spectra for I-IV are Mn L_3-edge RXES and those for V-VII are Mn L_2-edge RXES. The spectrum for VIII is off-resonant XES.

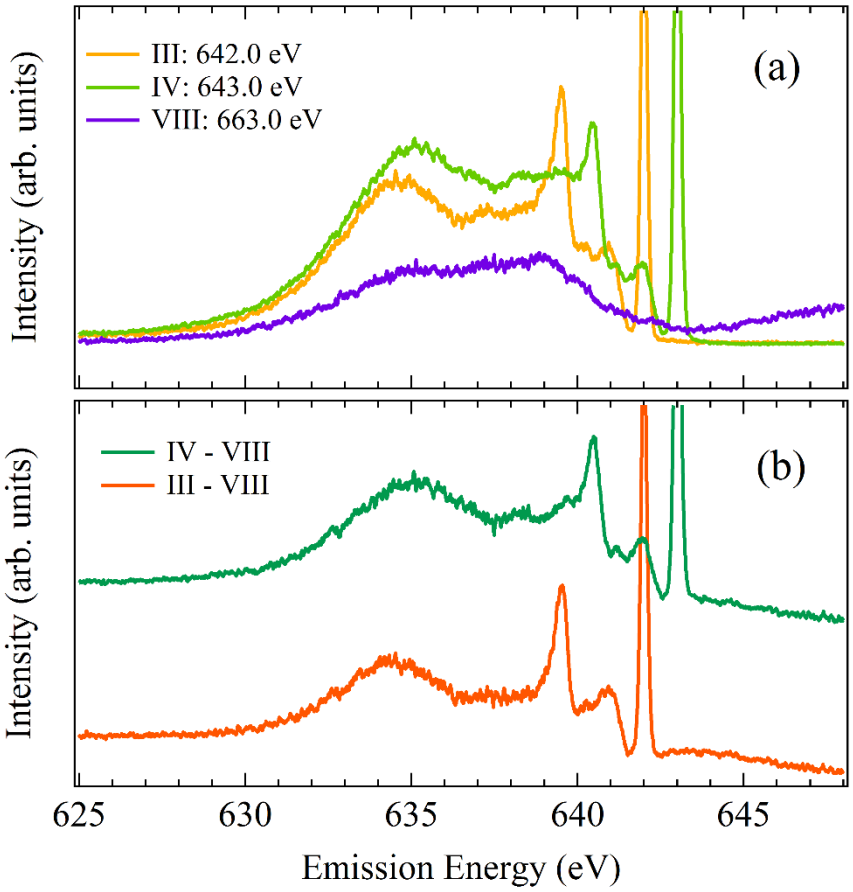

Fig. S2. (a) Comparison between the Mn L_3-edge RXES spectra and off-resonant XES spectrum in Fig. S1. (b) Difference spectra of III – VIII and IV – VIII. Note that the powder sample includes both the Mn^{3+} and Mn^{4+} states.

Parameter dependences for the CIFM calculation

We investigated the tendencies of "peak positions (particularly for the *dd* excitations)" and "peak heights" with varying several parameters (Figs. S3 and S4). The black spectra for Fig. S3 and the red spectra for Fig. S4 are determined as the best calculated results. We set the error bar for 10*Dq* to be ±0.15 eV, half of each step of the investigated values in Figs. S3 and S4 to assess the "best" parameter. For Δ and (*pd*σ), the peak positions of CT excitation are considered in addition to the *dd* excitation peaks. The error bars for Δ and (*pd*σ) are ±0.5 eV and ±0.1 eV, respectively using the same criteria as 10*Dq*.

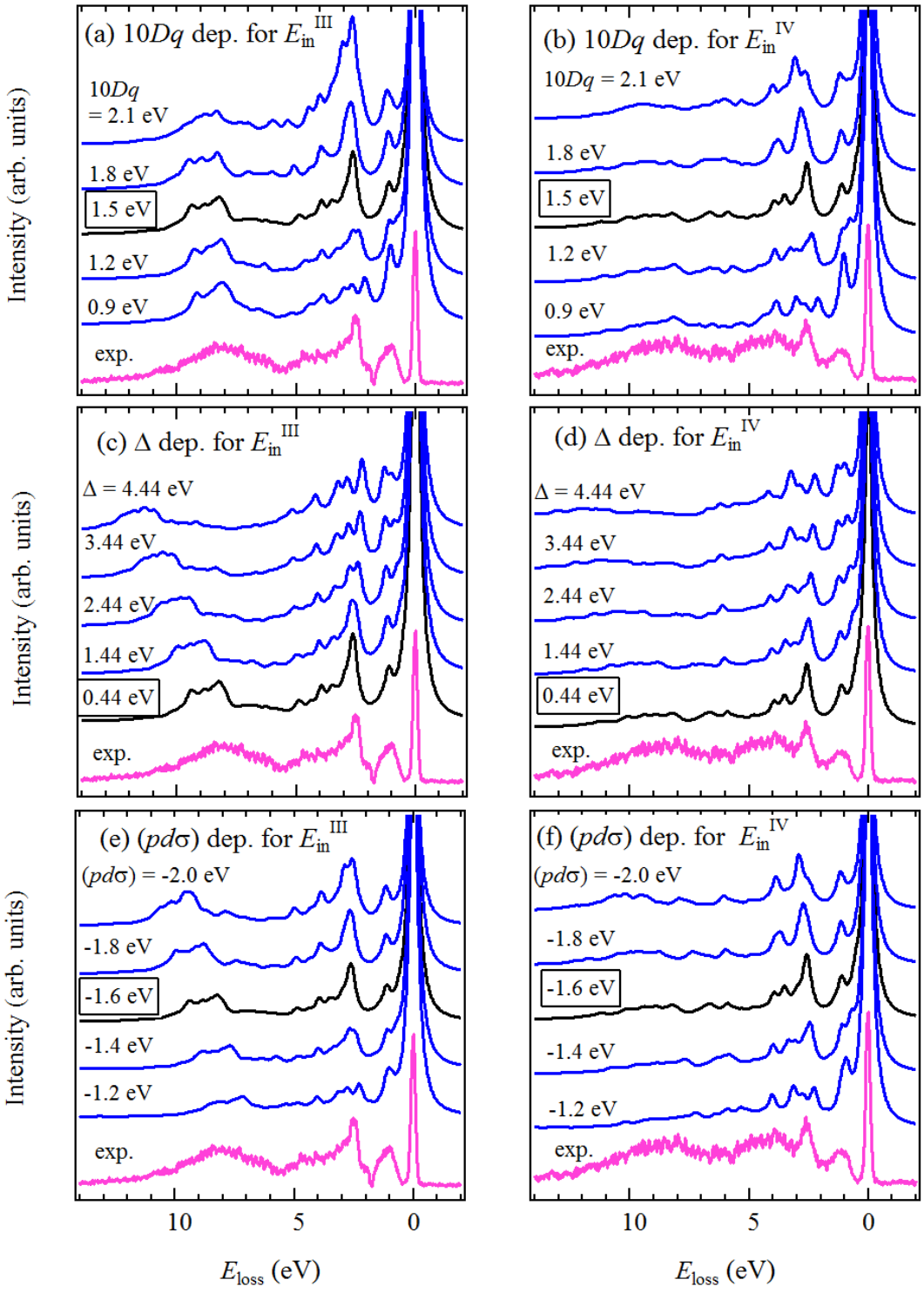

Fig. S3. Calculated XES spectra for Mn^{3+} state compared with the experimental difference spectra shown in Fig. 4 in text. (a) and (b), (c) and (d), and (e) and (f) show the $10Dq$, Δ and ($pd\sigma$) dependences, respectively. We determined the black spectra as the best calculated results.

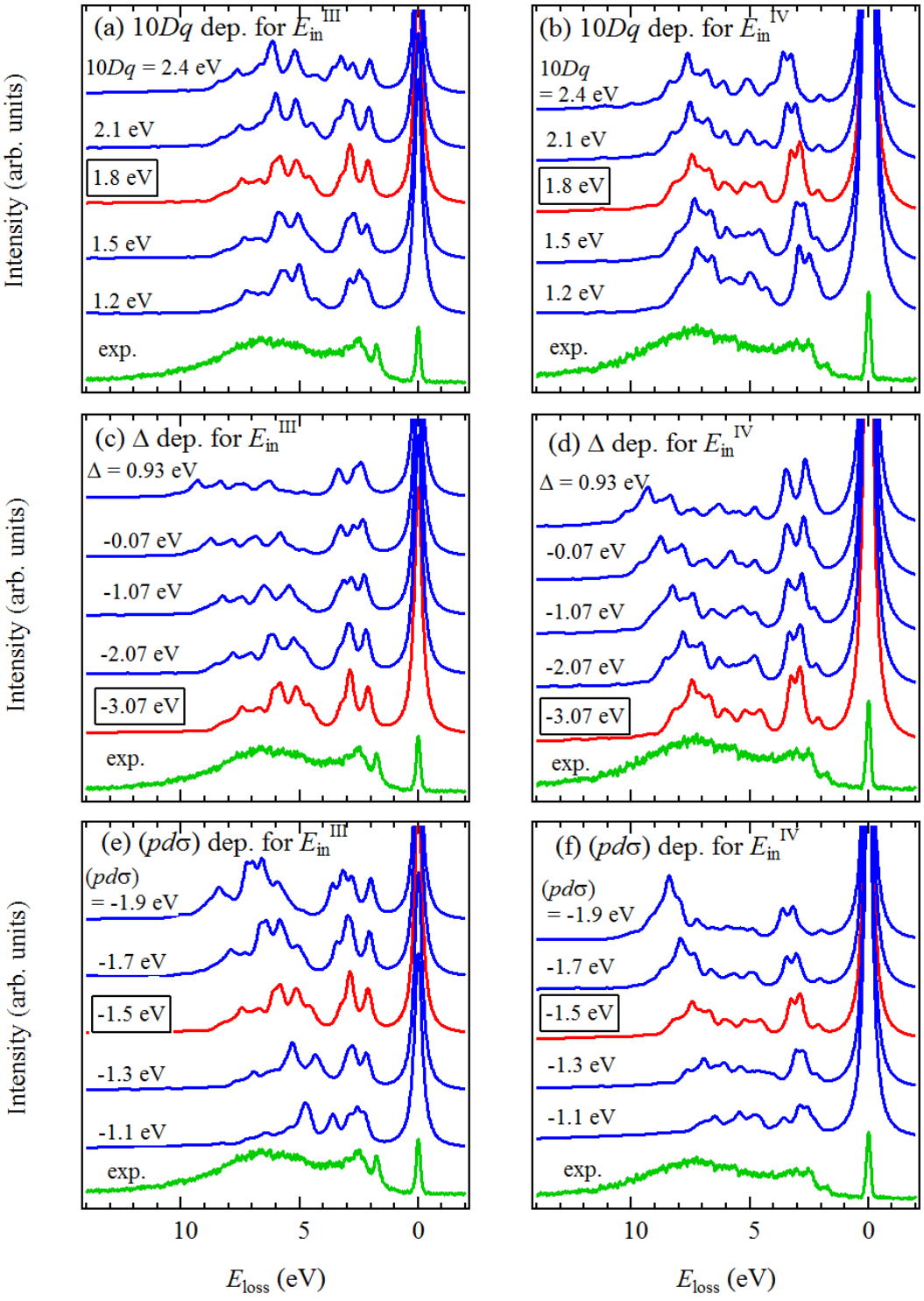

Fig. S4. Calculated XES spectra for Mn^{4+} state compared with the experimental charged spectra shown in Fig. 4 in text. (a) and (b), (c) and (d), and (e) and (f) show the 10*Dq*, Δ and (*pd*σ) dependences, respectively. We determined the red spectra as the best calculated results.

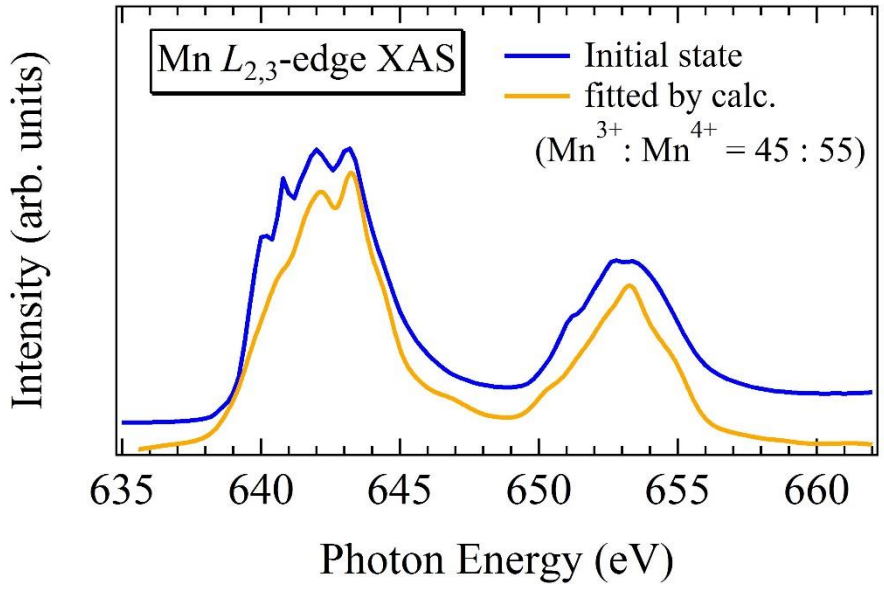

Fig. S5. The fitted XAS spectrum for the initial state using the calculated spectra (Fig. 6 in the main text) with a ratio of Mn^{3+} (calc.) : Mn^{4+} (calc.) = 45 : 55.

CIFM calculation for Mn^{3+} and Mn^{4+} states

For the CIFM calculation of the Mn $L_{2,3}$-edge XAS and Mn 2*p*-3*d*-2*p* RXES in $Li_xMn_2O_4$, we employed the octahedral $[MnO_6]^{y-}$ (y = 9, 8) cluster with the Hamiltonian as,

$$\mathcal{H} = \sum_{j,\gamma,\sigma} \varepsilon_P(j\gamma) n_{P,j\gamma\sigma} + \sum_{j,\gamma,\sigma} V_{pd}(j\gamma)\left(d^{\dagger}_{\gamma\sigma} P_{j\gamma\sigma} + h.c.\right) + \sum_{\gamma,\sigma}\left[\varepsilon_d(\gamma) - Q\sum_{m,\sigma'}\left(1 - n_{p,m\sigma'}\right)\right] n_{d,\gamma\sigma}$$
$$+ \sum_{m,\sigma} \varepsilon_{p,m\sigma} n_{p,m\sigma} + U\sum_{\gamma} n_{d,\gamma\uparrow} n_{d,\gamma\downarrow} + \sum_{\gamma>\gamma',\sigma,\sigma'} \left(U' - J\delta_{\sigma,\sigma'}\right) n_{d,\gamma\sigma} n_{d,\gamma'\sigma'} + \mathcal{H}_{multi}$$

where $d^{\dagger}_{\gamma\sigma}$ and $P^{\dagger}_{j\gamma\sigma}$ represent the Mn 3*d* and O 2*p* electron creation operator, in which spin σ is ↑ or ↓. While the symmetry γ is e_g or t_{2g} irreducible representation in Mn^{4+} configuration, that represents a_{1g}, b_{1g}, b_{2g}, and e_g irreducible representation in Mn^{3+} configuration. The number operators for Mn 3*d*, Mn 2*p*, and O 2*p* are $n_{d,\gamma\sigma}$ and $n_{p,m\sigma}$, and $n_{P,j\gamma\sigma}$, respectively, where *m* represents the magnetic quantum number. The first and second terms are the O 2*p* states and Mn 3*d*-O 2*p* hybridization, respectively. The third term describes the Mn 3*d* states with $\varepsilon_d(\gamma)$ being the one-electron energy level and *Q* being

the averaged Coulomb attraction caused by Mn 2*p* core hole. The fourth term is the Mn 2*p* states. The fifth and sixth terms represent the Coulomb and exchange interactions between Mn 3*d* electrons. The last term includes the multipole part of the Mn 3*d*- Mn 3*d* and Mn 3*d*- Mn 2*p* Coulomb interactions that are not described in the fifth and six terms and the spin-orbit interactions for the Mn 3*d* and Mn 2*p* orbitals. We evaluated the Slater integrals using Cowan's code[S1] and reduced them to 85% not considered in the present study.

The XES spectrum was calculated by the following expression[S2]:

$$I_{\mathrm{XES}}(\omega_{\mathrm{in}},\omega_{\mathrm{out}}) = \sum_f \left| \sum_m \frac{\langle f|T_\nu|m\rangle\langle m|T_\mu|g\rangle}{E_g+\omega_{\mathrm{in}}-E_m-i\Gamma} \right|^2 \delta(\omega_{\mathrm{out}}+E_f-\omega_{\mathrm{in}}-E_g)$$

Where ω_{in} and ω_{out} are the incident and emitted photon energy. $|g\rangle$, $|m\rangle$, and $|f\rangle$ represent the ground (initial), intermediate, and final state, respectively, and the corresponding energies are E_g, E_m, E_f. T denotes the electric dipole operator. The core-hole lifetime broadening effect in the intermediate state is taken into account with a constant parameter Γ for Mn 2*p* core-hole level. Since the XAS finale state corresponds with the XES intermediate one, the XAS spectrum was calculated using the Fermi's golden rule expressed as,

$$I_{XAS}(\omega_{in}) = \sum_m \left|\langle m|T_\mu|g\rangle\right|^2 \delta(\omega_{in}-E_m+E_g).$$

In the numerical calculation, the wave function was obtained by the Lanczos method.[S3] The theoretical line spectra thus obtained were convoluted, using Lorentzian and Gaussian functions (with each width of 0.6 eV).

The diagonal elements and CT energies used in this study are defined. In the octahedral $[MnO_6]^{8-}$ cluster, the CT energy from high-spin d^3 (t_{2g}^3) to $d^4\underline{L}(e_g)$ is given as

$$E\left[d^4\underline{L}\right] - E[d^3] = \Delta(\mathrm{Mn}^{4+}) + 6Dq - \varepsilon_P(e_g), \qquad \text{(S1)}$$

where $\varepsilon_P(e_g)$ is the O 2*p* state hybridized with 3*d*(e_g) orbitals. This value is 1.25 eV from the transfer integral value ($pp\sigma$). The energy of d^3 electron configuration is

$$E[d^3] = 3\varepsilon_d + 3U - 9J - 12Dq + E_0 \qquad \text{(S2)}$$

and

$$\Delta(\mathrm{Mn}^{4+}) = \varepsilon_d + 3U - 9J. \quad \text{(S3)}$$

The relation between U and the averaged Coulomb interaction $\bar{U}$ is expressed as

$$U = \bar{U} + 4F_2 + 36F_4 \quad \text{(S4)}$$

where F_2 and F_4 are the Slater integrals. In Eq. (S2), E_0 is the sum of the energies of Mn 2p electrons and those of ligand electrons. An one-electron energy ε_d is expressed as

$$\varepsilon_d = \frac{2\varepsilon_d(e_g)+3\varepsilon_d(t_{2g})}{5}. \quad \text{(S5)}$$

The octahedral crystal field splitting is $10Dq = \varepsilon_d(e_g) - \varepsilon_d(t_{2g})$. We also show the averaged CT energy Δ' (= $\varepsilon_d + 3\bar{U}$, for Mn^{4+}) in Table 1 of the main text for comparisons with previous studies.

In the tetragonal $[MnO_6]^{9-}$ cluster, the CT energy from high-spin d^4 ($a_{1g}b_{2g}e_g^2$) to $d^5\underline{L}(b_{1g})$ is given as

$$E\left[d^5\underline{L}\right] - E[d^4] = \Delta(\mathrm{Mn}^{3+}) + 6Dq - \tfrac{2}{7}B_0^2 - \varepsilon_P\left(b_{1g}\right), \quad \text{(S6)}$$

where $\varepsilon_P(b_{1g})$ is the O 2p state hybridized with 3d(b_{1g}) orbitals. This value is 1.25 eV from the transfer integral value $(pp\sigma)_{xy}$. The energy of d^4 electron configuration is

$$E[d^4] = 4\varepsilon_d + 6U - 18J - 6Dq + \frac{2}{7}B_0^2 + E_0 \quad \text{(S7)}$$

and

$$\Delta(\mathrm{Mn}^{3+}) = \varepsilon_d + 4U - 12J. \quad \text{(S8)}$$

An one-electron energy ε_d is expressed as

$$\varepsilon_d = \frac{\varepsilon_d(a_{1g})+\varepsilon_d(b_{1g})+\varepsilon_d(b_{2g})+2\varepsilon_d(e_g)}{5}. \quad \text{(S9)}$$

The tetragonal crystal field splitting is $B_0^2 = \frac{7}{4}(\varepsilon_d(a_{1g}) - \varepsilon_d(b_{1g}))$. The averaged CT energy Δ' (= $\varepsilon_d + 4\bar{U}$, for Mn^{3+}) is also shown in Table 1 of the main text. For the Mn^{3+} configuration, the transfer integrals for Mn-O and O-O, ($pd\sigma$) and ($pp\sigma$), includes the anisotropic hybridization. In reference to Ref. S4, the ratios of Mn-O and O-O interatomic distances along x-direction to those along z-direction are 0.936 and 0.966, respectively. Thus, we define $(pd\sigma)_z / (pd\sigma)_{xy} = 0.936^{3.5}$ and $(pp\sigma)_z / (pp\sigma)_{xy} = 0.966^{2.0}$. $(pd\sigma)_{xy}$ and $(pp\sigma)_{xy}$ represent the transfer integral in the xy-plane, which correspond with ($pd\sigma$) and ($pp\sigma$) in Table 1 in the text.

References

S1. R. D. Cowan, *The Theory of Atomic Structure and Spectra*; University of California Press: Berkeley, CA, 1981.

S2. F. de Groot and A. Kotani, *Core Level Spectroscopy of Solids*, Advances in Condensed Matter Science, CRC Press, Boca Raton, FL, 2008.

S3. V. Heine, *Solid State Physics*; H. Ehrenreich, F. Seitz, D. Turnbull, Eds.; Academic Press: New York, 1980; Vol. 35, p 87.

S4. C. Y. Ouyang, S. Q. Shi, and M. S. Lei, J. Alloy. Compd. **474**, 370-374 (2009).